

# A novel story on rock slope reliability, by an initiative model that incorporated the harmony of damage, probability and fuzziness

Yajun Wang \*

*School of Maritime and Civil Engineering, Zhejiang Ocean University, 1# Southern Road of Haida, Changzhi Island, Lincheng New District, Zhoushan City, Zhejiang Province, P.R. China*

*(Received November 28, 2015, Revised October 13, 2016, Accepted October 24, 2016)*

**Abstract.** This study aimed to realize the creation of fuzzy stochastic damage to describe reliability more essentially with the analysis of harmony of damage conception, probability and fuzzy degree of membership in interval [0,1]. Two kinds of fuzzy behaviors of damage development were deduced. Fuzzy stochastic damage models were established based on the fuzzy memberships functional and equivalent normalization theory. Fuzzy stochastic damage finite element method was developed as the approach to reliability simulation. The three-dimensional fuzzy stochastic damage mechanical behaviors of Jianshan mine slope were analyzed and examined based on this approach. The comprehensive results, including the displacement, stress, damage and their stochastic characteristics, indicate consistently that the failure foci of Jianshan mine slope are the slope-cutting areas where, with the maximal failure probability 40%, the hazardous Domino effects will motivate the neighboring rock bodies' sliding activities.

**Keywords:** fuzziness; stochastics; rock slope; damage; reliability

---

## 1. Introduction

Damage, by the help of uncertain theoretical models (Zhang and Valliappan 1990a, b, Silberschmidt and Chabochej 1994, Silberschmidt 1998, Zhang and Valliappan 1998a, b), nowadays shows new genius in geo-engineering work; Ju and Tseng (1995), based on micro-mechanics and mean-volume theory, investigated the mechanical characters of brittle material that was planted with plane grain cracks obeying correlative random distribution; Rinaldi *et al.* (2007) introduced one semi-empirical calculation model to simulate statistical damage. Some excellent work has also been done to study the uncertainty of damage. However, most of these work adopted the single uncertain math model (Dzenis 1993, 1996, Ihara and Tanaka 2000, Bulleit 2004). Stochastics was the most popular theory for damage study in the past (Zeitoun and Baker 1992). Fuzziness on damage was omitted. Actually, both the definition and the computation on damage have the logically fuzzy characteristics (Rigatos and Zhang 2009, Rezaei *et al.* 2011). Damage has also been applied in geo-engineering for a long time because the reliability of geo-subjects could be analyzed based on damage theory (Yang and Pan 2015). There is still little work to discuss the intrinsic fuzziness and stochastics of damage and reliability on geo-engineering.

Thus, a fuzzy stochastic damage model was developed in this study and it was implemented in

---

\*Corresponding author, Ph.D., E-mail: [aegis68004@163.com](mailto:aegis68004@163.com)

reliability analyses for one mine slope in China.

## 2. Stochastic distribution of damage variable

It has been generally accepted that damage variable  $\Omega$  has a stochastic nature.

Stochastic damage variable shows  $\beta$  distribution in some work (Zhang and Valliappan 1990a, b, 1998a, b).

Thus, the stochastic damage variable can be established in random space  $\Psi$  as

$$\begin{aligned} \Omega \in \Lambda_{\alpha'}, \quad \Lambda_{\alpha'} = \{U_{\alpha'}, e_{\alpha'}, \sigma_{\alpha'}, f_{\alpha'}\}, \\ \cup_{\alpha' \in X} \Lambda_{\alpha'} \subset \Psi \quad (\alpha' \in X = (x_1, x_2, \dots, x_n)^T) \end{aligned} \quad (1)$$

where  $\alpha'$  is a stochastic subset of stochastic vector  $X = (x_1, x_2, \dots, x_n)^T$  and  $x_i$  represents the stochastic parameter of the target materials;  $n$  is the size of stochastic parameters; the superscript “ $T$ ” denotes the transposed operator;  $\Lambda_{\alpha'}$  is a probabilistic set derived from  $\alpha'$ , consisting of probabilistic nodal displacement vector  $U_{\alpha'}$ , stochastic strain tensor  $e_{\alpha'}$ , stochastic stress tensor  $\sigma_{\alpha'}$  and probabilistic body force vector  $f_{\alpha'}$ .

The crucial propositions are provided below:

Proposition 1:  $\Psi_1$  is defined as a probabilistic space of independent  $\beta$  distribution, and  $[0, 1]$  is defined as the domain of stochastic vector  $x$  from  $\Psi_1$ . The relation is expressed as  $x \rightarrow \beta(p, q)$ :  $\Psi_1|x = [0, 1]$ , where  $\beta(p, q)$  is the  $\beta$  distribution function, and  $p$  and  $q$  are the parameters for  $\beta$  function. Therefore,  $\Psi_1$  is a Banach space under the  $\infty$  norm, or a complete normed linear space.

Meanwhile, the  $\beta$  probabilistic cumulative distribution function vector can be defined as  $y_1$ .  $\Psi_2$  is defined as a probabilistic space of damage variable  $\Omega$ , which shows independent  $B$  distribution over  $[0, 1]$ , i.e.,  $\Omega \rightarrow B$ :  $\Psi_2|\Omega = [0, 1]$ . Following the same rule, it can be proven under the  $\infty$  norm definition that this is a Banach space, which can be expressed as  $\Omega \rightarrow B$ :  $\Psi_2|\Omega = [0, 1]$ . Meanwhile, the  $B$  probabilistic cumulative distribution function vector can be defined as  $y_2$ .

Proposition 2: The necessary and sufficient condition for coincidence of the probabilistic spaces  $\Psi_1$  and  $\Psi_2$  is that vector  $y_2$  converges to vector  $y_1$  with the same definition domain  $[0, 1]$  under the  $\infty$  norm. The propositions have been proved by Wang (2012).

Based on proposition 1 & 2,  $\beta$  distribution can be used to simulate  $B$  distribution of damage variable  $\Omega$ , and this procedure can be applied to engineering through the law of averages over  $[0, 1]$ .

## 3. Fuzzy membership of damage variable

The damage of materials or structures, under various factors (internal or external ones), is a physical-mechanical process from the development and evolution of micro-defects to macro-behaviors whose performances are the engineers' interests (including materials' deformation and structures' failure etc). Therefore, the definition of damage should incorporate the macro-effects produced by the development and evolution of micro-defects. A quantitative index  $\varpi$  that can quantify the material's micro-defects is called a damage measuring index (DMI).  $\Gamma$  is a fuzzy analytical domain for  $\varpi$ , i.e.,  $\varpi \in \Gamma$ .  $\Gamma$  must be defined in a fuzzy space  $\Xi(\tilde{C}, \tilde{L}, \tilde{P})$ , where  $\tilde{C}$ ,  $\tilde{L}$  and  $\tilde{P}$  represent the fuzziness of physical parameters (including  $\Omega$ ), loading conditions, and

boundary conditions, respectively. Then, the key technology for damage simulation is which scale of  $\varpi$  means the material's damage or how  $\varpi$  rates damage. This essential mechanism describes the fuzziness of  $\varpi$  evolution.  $\Omega$ , as a fuzzy functional on  $\varpi$ , represents the magnitude of the membership value of  $\varpi$  for domain  $\Gamma$ , and can analyze damage variable development as

$$\Omega = \varsigma_{\varpi \in \Gamma}[\omega(\varpi)] = \omega_{\Gamma}(\varpi) \tag{2}$$

where  $\varsigma_{\varpi \in \Gamma}$  is a fuzzy membership functional, namely,  $\varpi \in \Gamma : \tilde{A} \subset \Xi(\tilde{C}, \tilde{L}, \tilde{P}) | \Omega \in [0, 1]$ ;  $\tilde{A}$  is the fuzzy subset in domain  $\Gamma$  and includes three kinds of fuzziness represented by  $\tilde{C}, \tilde{L}$  and  $\tilde{P}$ ;  $\omega$  is the generalized probabilistic integral variable on  $\varpi$ ; and  $\omega_{\Gamma}$  is the function on the generalized probabilistic integral variable.

Modulus degradation computation was often used as the approach of 'damage' definition (Hearndon *et al.* 2008, Vili *et al.* 2014). However, this approach has an inconvenience in incorporating the development of mechanical fields, such as stress, strain and displacement etc. Therefore, the study point of our work is that the damage measuring index should incorporate as much and direct information on the development of mechanical fields of engineering cases as possible. We defined the evolution of volumetric deformation and torsional deformation as the main resource of damage development. The evolution of volumetric stress and deviatoric stress can represent their development directly (Bolton *et al.* 2008). We used the strength expression to explain the volumetric stress evolution of geo-material. The invariable of the deviatoric stress tensor was computed here to explain the evolution of torsional deformation of geo-material. Thus, our study defined DMI as

$$\varpi = \frac{|\sigma_m| \tan \varphi + c}{(J_2)^{\frac{1}{2}}} \tag{3}$$

where  $\varphi$  and  $c$  are the internal friction angle and cohesive strength, respectively;  $\sigma_m$  and  $J_2$  are the hydrostatic pressure and the second invariable of the deviatoric stress tensor, respectively.

The linear fuzzy memberships functional are the preferences of engineering cases (MahdaviFar 2000). Therefore, two linear cases are considered in the fuzzification for  $\varpi$  and the fuzzy memberships functional are explained as: (1) torsional deformation is superior to volumetric deformation in magnitude when material damage is developing (Eq. (4); Fig. 1, line a); (2) volumetric deformation is superior to torsional deformation in magnitude when material damage is developing (Eq. (5); Fig. 1, line b).

$$\Omega = \begin{cases} 1 & 0 \leq \varpi \leq a \\ \frac{b - \varpi}{b - a} & a < \varpi \leq b \\ 0 & \varpi > b \end{cases} \tag{4}$$

$$\Omega = \begin{cases} 1 & 0 \leq \varpi \leq b' \\ \frac{\varpi - b'}{a' - b'} & b' < \varpi \leq a' \\ 1 & \varpi > a' \end{cases} \tag{5}$$

where  $a, a', b$  and  $b'$  are tests' parameters.

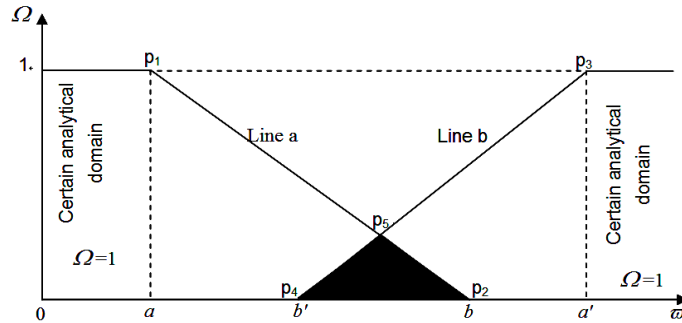


Fig. 1 Fuzzy memberships functional

Thus, there is linear relation between  $w$  and  $\Omega$  from  $\Omega = 0$  to  $\Omega = 1$ . Here, lines  $a$  and  $b$  in Fig. 1 have two characteristic points (i.e.,  $p_1, p_2, p_3$  and  $p_4$ ), respectively. By the help of line  $\Omega = 1$  and axis  $w$ , these characteristic points can be fixed according to the tests' data. Hence, these tests' parameters can be ascertained. Fuzzy memberships functional Eqs. (4) and (5) have somewhat overlap zone (triangular area  $p_2p_4p_5$ ). Hence, they have super fuzzy robustness (Farkas *et al.* 2010).

The damage development of engineering cases is such a complicated problem that both volumetric deformation and torsional deformation may activate it and cause the eventual failure of material or structure (Pine *et al.* 2007). Therefore, Eqs. (4)-(5) will be used together during the computation of damage and the de-fuzzification for them will be implemented for reliability analysis.

#### 4. Fuzzy stochastic damage variable

When fuzziness and stochastics exist simultaneously in the damage evolution process, according to the expansion criterion, the single fuzzy space  $\Xi$  and single random space  $\Psi$  need to be expanded to a generalized uncertain space  $O: \zeta(s, f), U_{s,f}, e_{s,f}, \sigma_{s,f}, f_{s,f} \subset O: \zeta(s, f)$ , where  $s$  and  $f$  are the stochastic coverage and fuzzy coverage, respectively;  $\zeta(s, f)$  is the subset of generalized uncertain space;  $U_{s,f}$  is the fuzzy stochastic nodal displacement vector;  $e_{s,f}$  is the fuzzy stochastic strain tensor;  $\sigma_{s,f}$  is the fuzzy stochastic stress tensor;  $f_{s,f}$  is the fuzzy stochastic body force vector.

The generalized cumulative distribution function (GCDF)  $F_{\Omega}^f$  and generalized probabilistic density function (GPDF)  $f_{\Omega}^f$  obtained by the expansion criterion and fuzzy probabilistic integration are the functions of fuzzy memberships functional on  $\Omega$ . According to Eqs. (4)-(5), the GCDF and GPDF can be established based on the definition of DMI as

$$F_{\Omega}^f(\Omega) = \frac{1}{\beta(p, q)} \int_0^{\Omega} \omega^{p-1} (1-\omega)^{q-1} \mu_{w \in \Gamma}[\omega(w)] d\omega$$

$$= \begin{cases} \frac{1}{\beta(p, q)} \int_0^{\Omega} \omega^{p-1} (1-\omega)^{q-1} \cdot 1 d\omega & 0 \leq w \leq a \\ \frac{1}{\beta(p, q)} \int_0^{\Omega} \omega^{p-1} (1-\omega)^{q-1} \left( \frac{b-w}{b-a} \right) d\omega & a < w \leq b \\ 0 & w > b \end{cases} \tag{6}$$

$$\begin{aligned}
 f_{\Omega}^f(\Omega) &= \frac{1}{\beta(p,q)} \Omega^{p-1} (1-\Omega)^{q-1} \mu_{\varpi \in \Gamma}[\omega(\varpi)] \\
 &= \begin{cases} 1 & 0 \leq \varpi \leq a \\ \frac{1}{\beta(p,q)} \Omega^{p-1} (1-\Omega)^{q-1} \left( \frac{b-\varpi}{b-a} \right) & a < \varpi \leq b \\ 0 & \varpi > b \end{cases} \quad (7)
 \end{aligned}$$

$$\begin{aligned}
 F_{\Omega}^f(\Omega) &= \frac{1}{\beta(p,q)} \int_0^{\Omega} \omega^{p-1} (1-\omega)^{q-1} \mu_{\varpi \in \Gamma}[\omega(\varpi)] d\omega \\
 &= \begin{cases} 0 & 0 \leq \varpi \leq b' \\ \frac{1}{\beta(p,q)} \int_0^{\Omega} \omega^{p-1} (1-\omega)^{q-1} \frac{\varpi-b'}{a'-b'} d\omega & a < \varpi \leq b \\ \frac{1}{\beta(p,q)} \int_0^{\Omega} \omega^{p-1} (1-\omega)^{q-1} .1 d\omega & \varpi > b \end{cases} \quad (8)
 \end{aligned}$$

$$\begin{aligned}
 f_{\Omega}^f(\Omega) &= \frac{1}{\beta(p,q)} \Omega^{p-1} (1-\Omega)^{q-1} \mu_{\varpi \in \Gamma}[\omega(\varpi)] \\
 &= \begin{cases} 0 & 0 \leq \varpi \leq b' \\ \frac{1}{\beta(p,q)} \Omega^{p-1} (1-\Omega)^{q-1} \left( \frac{\varpi-b'}{a'-b'} \right) & b' < \varpi \leq a' \\ \frac{1}{\beta(p,q)} \Omega^{p-1} (1-\Omega)^{q-1} .1 & \varpi > a' \end{cases} \quad (9)
 \end{aligned}$$

The GCDF and GPDF are the key tools for the numerical computation in standard normal space only where the reliability of engineering cases can be analyzed precisely.

### 5. Damage reliability with fuzziness & stochastics

Fuzzy stochastic damage reliability simulation here was realised based on fuzzy stochastic damage finite element method. Drucker-Prager (D-P) constitutive model was assimilated into fuzzy stochastic damage finite element method. The key constitutive component for the methodology is the ultimate status function gradient  $\nabla g_{\alpha^*}$ , which can be expressed as

$$\nabla g_{\alpha^*}(Y^*) = \left( \frac{\partial g_{\alpha^*}}{\partial y_1^*}, \frac{\partial g_{\alpha^*}}{\partial y_2^*}, \dots, \frac{\partial g_{\alpha^*}}{\partial y_n^*} \right)^T \quad (10)$$

where  $Y^* = (y_1^*, y_2^*, \dots, y_n^*)^T$  is the independent standard normal stochastic vector;  $g_{\alpha^*}$  represents

the ultimate status function;  $\nabla$  is gradient operator.

Fuzzy stochastic damage finite element method will be implemented by iterative technique. The fastest iterative direction is the negative gradient direction defined by  $\alpha$  that can be computed by

$$\alpha = -\nabla g_{\alpha^*}(Y^*) / \|\nabla g_{\alpha^*}(Y^*)\| \quad (11)$$

where  $\|\cdot\|$  is a Euclidean norm operator.  $\|\nabla g_{\alpha^*}(Y^*)\|$  can be calculated by

$$\|\nabla g_{\alpha^*}(Y^*)\| = \sqrt{\left(\frac{\partial g_{\alpha^*}}{\partial y_1^*}\right)^2 + \left(\frac{\partial g_{\alpha^*}}{\partial y_2^*}\right)^2 + \dots + \left(\frac{\partial g_{\alpha^*}}{\partial y_n^*}\right)^2} \quad (12)$$

$\alpha_i$  ( $i = 1, \dots, n$ ) (component of  $\alpha$ ) is the direction cosine of the reliability index along axis  $y_i^*$ . Thus,  $\alpha$  is perpendicular to the ultimate status surface against the coordinate system origin (the shortest iterative path here). The computed variables of reliability analyses including  $g_{\alpha^*}(Y^*)$  will converge the fastest to their stable values when the fuzzy stochastic damage finite element method is carried out iteratively along the negative gradient direction.

Then, the iterative step size of the numerical approach,  $d$ , can be determined by

$$d = g_{\alpha^*}(Y^*) / \|\nabla g_{\alpha^*}(Y^*)\| \quad (13)$$

In order to ensure the line connecting the origin of the  $k$ th iterative step on  $(Y^*)_k$  and the new iterative coordinate  $(Y^*)_{k+1}$  along the very negative gradient direction of the spatial curve, the updating for  $(Y^*)_k$  is the crucial technique for the numerical approach and can be expressed as

$$(Y^*)_{k'} = [(Y^*)_k]^T \alpha \alpha \quad (14)$$

where  $(Y^*)_{k'}$  is the updated expression on  $(Y^*)_k$ .

Therefore, the controlling iterative function can be deduced as

$$(Y^*)_{k+1} = \left\{ [(Y^*)_k]^T \alpha + \frac{g_{\alpha^*}(Y^*)}{\|\nabla g_{\alpha^*}(Y^*)\|} \right\} \alpha \quad (15)$$

Thus, the fuzzy stochastic damage reliability index  $\beta^*$  and failure probability  $P_f^*$  can be computed by

$$\beta^* = \sqrt{(Y^*)^T Y^*} = \sqrt{(y_1^*)^2 + (y_2^*)^2 + \dots + (y_n^*)^2} \quad (16)$$

$$P_f^* = 1 - \Phi(\beta^*) \quad (17)$$

## 6. Numerical algorithm with fuzziness & stochastics

It is very important that the stochastic vector  $X = (x_1, x_2, \dots, x_i, \dots, x_n)^T$  can't be used as direct



orthogonalization transformation matrix.

Hence, the independent non-standard stochastic vector  $Z = (z_1, z_2, \dots, z_i, \dots, z_n)^T$ , its expectation vector  $E$  and its ‘covariance matrix’  $D$  can be computed with matrixes  $C$  and  $H$

$$Z = H^T X \tag{22}$$

$$E = H^T X' \tag{23}$$

$$D = H^T CH \tag{24}$$

where the expectation vector  $E$  can be expressed as  $(\mu_1, \mu_2, \dots, \mu_i, \dots, \mu_n)^T$ ; the elements in the principal diagonal of  $D$  are the variances of  $Z$  (i.e.,  $(\delta_{z_1}^2, \delta_{z_2}^2, \dots, \delta_{z_i}^2, \dots, \delta_{z_n}^2)^T$  where  $\delta_{z_i}$  is the mean square deviation of  $z_i$ ) and they are positive real; other elements are zeroes. Therefore, the so-called ‘covariance matrix’  $D$  is the diagonal one actually and all the nonzero elements are the very variances of  $Z$ . The procedure can be named as independence orthogonalization.

Furthermore, the independent non-standard stochastic vector  $Z = (z_1, z_2, \dots, z_i, \dots, z_n)^T$  needs to be standardized. The standardization procedure can be expressed as

$$Y^* = TZ + B \tag{25}$$

where transformation matrix  $T$  is computed by

$$T = \begin{bmatrix} \frac{1}{\delta_{z_1}} & & & & 0 \\ & \frac{1}{\delta_{z_2}} & & & \\ & & \dots & & \\ & & & \frac{1}{\delta_{z_i}} & \dots \\ & & & & \dots & \frac{1}{\delta_{z_n}} \\ 0 & & & & & & 0 \end{bmatrix} \tag{26}$$

and the transformation vector  $B$  is computed by

$$B = \left( -\frac{\mu_{z_1}}{\delta_{z_1}}, -\frac{\mu_{z_2}}{\delta_{z_2}}, \dots, -\frac{\mu_{z_i}}{\delta_{z_i}}, \dots, -\frac{\mu_{z_n}}{\delta_{z_n}} \right)^T \tag{27}$$

where  $Y^*$  is the independent standard normal stochastic vector. Then, the reliability analyses on fuzzy stochastic damage field can be implemented in the  $n$ -dimension standard normal space that can be formed by  $V^* = (v_1^*, v_2^*, \dots, v_i^*, \dots, v_n^*)^T$

Damage variable  $\Omega$  from  $Y^* = (y_1^*, y_2^*, \dots, y_i^*, \dots, y_n^*)^T$  must be de-fuzzified. The method is gravity model approach which can be expressed as

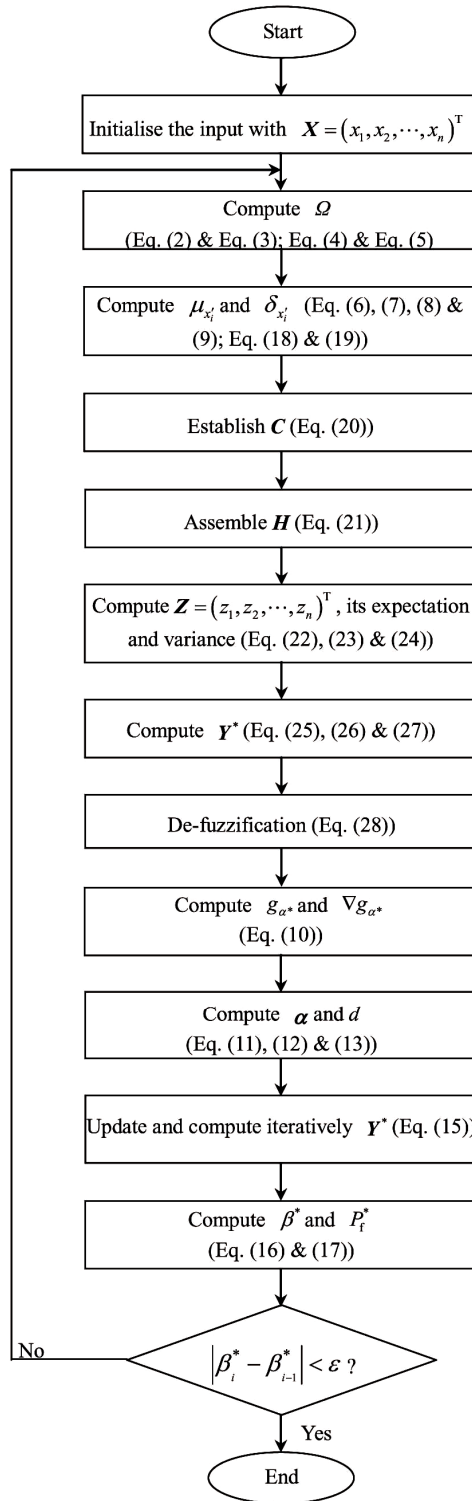


Fig. 2 Flowchart of iterative procedure for fuzzy stochastic damage finite element method

$$\Omega = \frac{\sum_{i=1}^N (\varpi \zeta_{\varpi \in \Gamma}^i)}{\sum_{i=1}^N \zeta_{\varpi \in \Gamma}^i} \quad (28)$$

where  $\zeta_{\varpi \in \Gamma}$  is the fuzzy membership functional on  $\varpi$ ;  $N$  is the size of fuzzy memberships functional. The gravity model approach has super robustness and is the most acceptable way for de-fuzzification.

The fuzzy stochastic damage reliability index  $\beta^*$  and failure probability  $P^*$  can be computed iteratively based on Eq. (15) until the converging condition  $|\beta_i^* - \beta_{i-1}^*| < \varepsilon$  is met. Here,  $\beta_{i-1}^*$  and  $\beta_i^*$  are the values of  $\beta^*$  at iterative step  $i-1$  and  $i$ , respectively.  $\varepsilon$  is the accuracy of the numerical analyses which is defined by the volume ratio of the minimal element over the total volume of the mesh.

The iterative procedure for the numerical approach is shown graphically in the flowchart of Fig. 2.

## 7. Examination and application

The fuzzy stochastic damage model will be examined and applied for the reliability analyses on the rock slope of Jianshan mine. Gravity is the main load for the reliability analyses.

Jianshan mine, standing in Shanxi province of Northern-Western China, is one of the greatest strip iron mines in China. Some colossal rock slopes have been formed during the long-term excavation from 1994. The maximal height of these slopes is 532 m.

Fig. 3(a) shows the finite element grid model for one typical rock slope of Jianshan mine and the rock slope height here is 400 m. The thickness of this typical rock slope section is 200 m. The slope-cutting areas are circled and labeled. The boundary conditions include: BC1 whose translation alongside principal axis  $x$  is constrained; BC2 whose translation alongside principal axis  $z$  is constrained; BC3 whose translation and rotation on three principal axes (i.e.,  $x$ ,  $y$  and  $z$ ) are constrained absolutely (Fig. 3(b)-(c)).

The rock slope consists of 6 high-angle strata, i.e., chlorite (AH), quartz (AQ), ferrous schist (AT), iron ore (FE), plagioclase schist (MDAT) and syenite stratum (SIGM) (in Fig. 4).

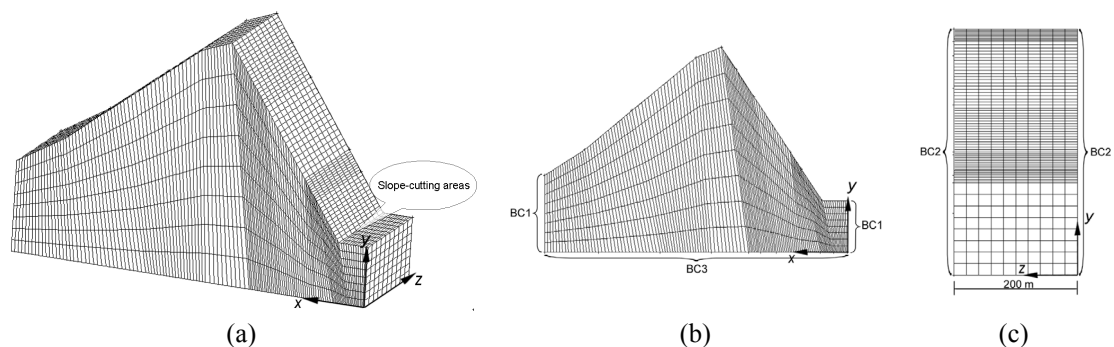


Fig. 3 Finite-element mesh of typical rock slope in Jianshan mine

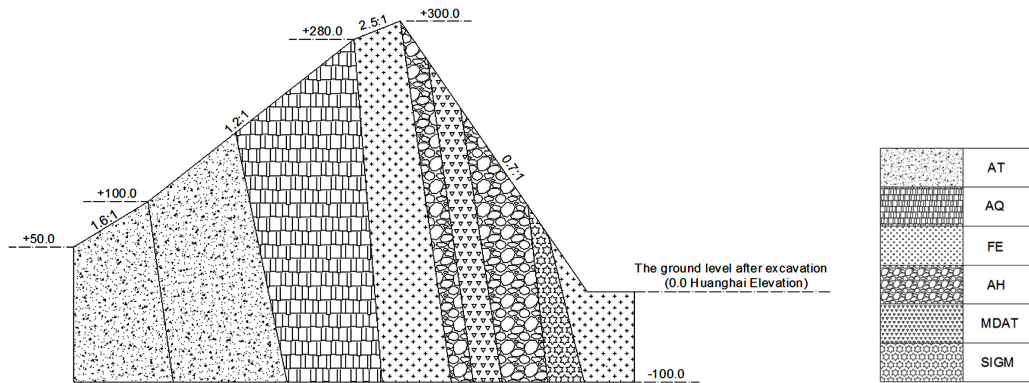


Fig. 4 Strata of typical rock slope in Jianshan mine

Table 1 Expectation values of strata materials parameters

Material number	Lithological series	Material code	Decay status	Young's modulus $E$ : kPa	Poisson ratio $\nu$	$c$ : kPa	$\varphi$ : degrees	Unit weight $\gamma$ : kN/m <sup>3</sup>
1	Chlorite	AH	Weathered	$1.20 \times 10^6$	0.37	3500	13	26.6
			Fresh	$5.42 \times 10^7$	0.27	3600	11	29.7
2	Quartz	AQ	Weathered	$6.70 \times 10^6$	0.26	3200	19	26.4
			Fresh	$5.41 \times 10^7$	0.22	3280	18	27.5
3	Ferrous schist	AT	Weathered	$2.96 \times 10^7$	0.37	3410	15	27.6
			Fresh	$4.69 \times 10^7$	0.26	3500	14	31
4	Iron ore	Fe	Moderately weathered	$5.59 \times 10^7$	0.27	2650	26	32
			Fresh	$6.21 \times 10^7$	0.2	2760	24	33
5	Plagioclase schist	MDAT	Moderately weathered	$2.18 \times 10^7$	0.29	2900	22	29
			Fresh	$6.01 \times 10^7$	0.24	3000	21	29.6
6	Syenite	SIGM	Weathered	$2.10 \times 10^7$	0.28	2780	23	29.7
			Fresh	$6.10 \times 10^7$	0.21	3010	20	29.8

Table 2 Variation values of strata materials parameters

Material number	$E$	$\nu$	$c$	$\varphi$	$\gamma$
1	0.09	0.06	0.23	0.09	0.04
2	0.07	0.08	0.24	0.05	0.08
3	0.09	0.06	0.23	0.04	0.11
4	0.09	0.07	0.31	0.03	0.08
5	0.09	0.07	0.26	0.05	0.07
6	0.09	0.06	0.28	0.03	0.10

Table 3 Correlation coefficients of strata material parameters

$\rho_{x_i x_j}$	$E$	$\nu$	$c$	$\varphi$	$\gamma$
$E$	1	0.3	0.13	0.5	0.29
$\nu$	0.3	1	0.41	0.72	0.11
$c$	0.13	0.41	1	0.64	0.53
$\varphi$	0.5	0.72	0.64 <td 1	0.105	
$\gamma$	0.29	0.11	0.53	0.105	1

The values in Tables 1-2 are the expectation and variation values of these rock strata materials parameters, respectively. The correlation coefficients of them are shown in Table 3.

For the clarification, the mechanical fields are expressed by the slicing images from the three-dimensional simulation results. The slicing position is at the middle point of the thickness of this typical rock slope section, namely,  $z = 100$ . The displacement fields are shown in Figs. 5-7. They can express the distribution characters of displacement without damage development under the gravity loading condition (Zhao *et al.* 2015).

The displacement values in the slope-cutting areas are very high and the contour distribution here is concentrative, too.

The main causes for this phenomenon are: there has been large relaxation during earlier excavation in the slope-cutting areas; the slope-cutting areas neighbors with the syenite stratum whose bulk specific gravity has great variation value; the high level of bulk specific gravity variation activates the unreliability of the slope-cutting areas (Schuster *et al.* 2008).

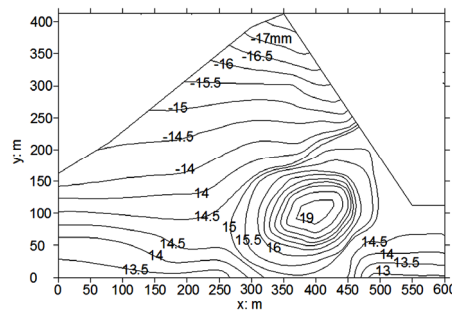


Fig. 5 Contour of  $x$ -displacement at cross-section without damage development

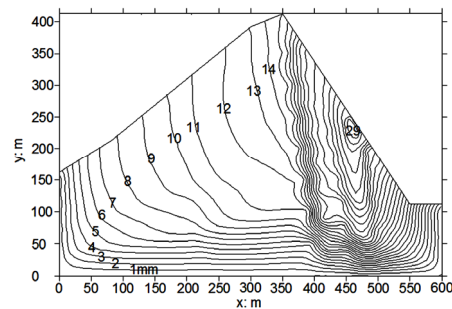


Fig. 6 Contour of  $y$ -displacement at cross-section without damage development

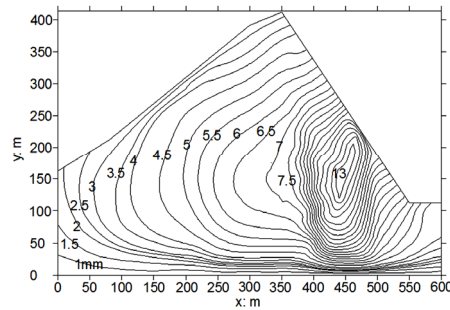


Fig. 7 Contour of z-displacement at cross-section without damage development

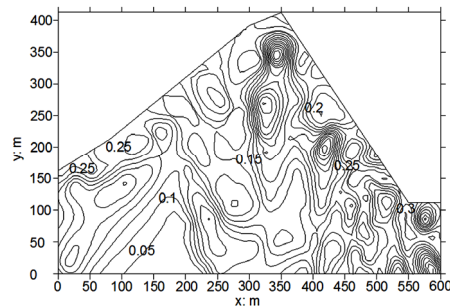


Fig. 8 Contour of expectation of damage variable at cross-section before equivalent normalization

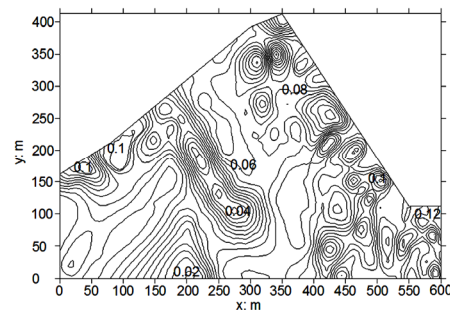


Fig. 9 Contour of expectation of damage variable at cross-section after equivalent normalization

According to Figs. 8-9, the expectation values of the damage variable diminish evidently after the parameters are equivalently normalized.

The levels of expectation values of the damage variable in the slope-cutting areas, whatever before or after equivalent normalization, are higher than that in other areas of the rock slope (Figs. 8-9). The results consist with that in Figs. 5-7. According to Figs. 8-9, the fuzzy stochastic damage numerical approach based on  $\beta$  distribution model is the conservative simulation on reliability analyses. Thus, the fuzzy stochastic damage reliability is applicable for geo-engineering because the simulation results have high degree of security.

Fig. 10 shows that the level of the mean square deviation of the damage variable is high in the slope-cutting areas (Chowdhury *et al.* 1987). These facts demonstrate that materials of these areas

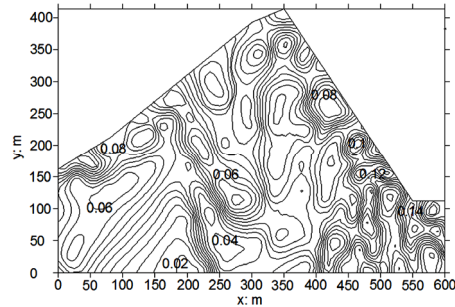


Fig. 10 Contour of mean square deviation of damage variable at cross-section after equivalent normalization

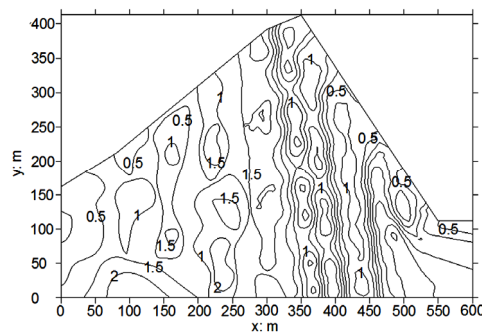


Fig. 11 Contour of  $\beta^*$  at cross-section after equivalent normalization

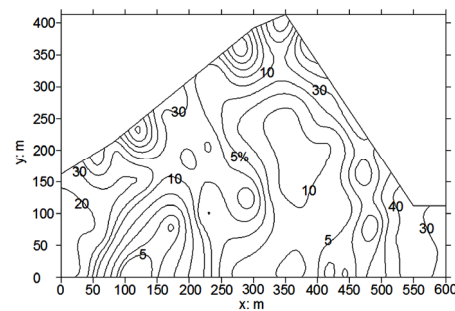


Fig. 12 Contour of  $P_f^*$  at cross-section after equivalent normalization

are vulnerable to be fractured due to the development of damage.

According to Fig. 11, there are different levels of reliability in every stratum of the rock slope because the strength and mechanical state of these strata are absolutely different.

Especially, the rock slope has very low level of reliability generally in those areas where the damage discreteness has great magnitude (including the slope-cutting areas). The results consist with that in Figs. 8-10. Namely, the high level of damage discreteness will cause the unreliability of materials and structures. This objective phenomenon can be shown and explained by the fuzzy stochastic damage reliability approaches.

Failure probability  $P_f^*$  is helpful for engineers to assess efficiently the macro-safety state of

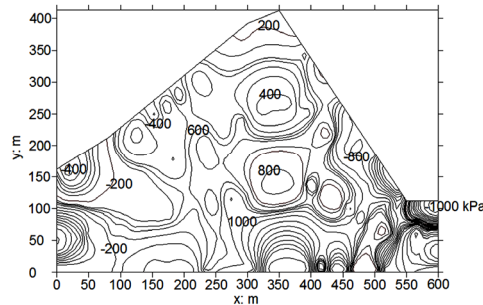


Fig. 13 Contour of expectation of  $\sigma_{xx}$  at cross-section after equivalent normalization

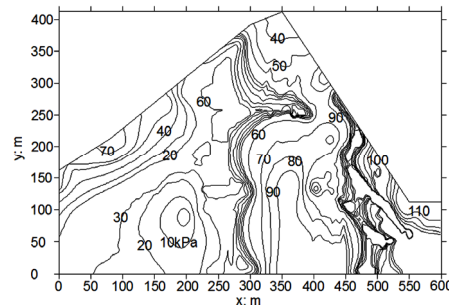


Fig. 14 Contour of variance of  $\sigma_{xx}$  at cross-section after equivalent normalization

engineering cases. Fig. 12 shows the macro-safety state of Jianshan mine slope. The slope-cutting areas have higher failure probability than other areas. The maximal failure probability here attains 40%.

The expectation and variance of fuzzy stochastic damage stress field (e.g., the results on principal axis  $x$ ) are shown by Figs. 13-14, respectively.

The maximal tensile stress (i.e., the maximal negative stress) lives in the slope-cutting areas (Fig. 13). Due to the facts, the rock slope here has lower reliability values. The results also consist with that in Figs. 11-12.

According to the distribution in this figure, there is a generally high level of discreteness of fuzzy stochastic damage stress in the slope-cutting areas where the fuzzy stochastic damage stress also accumulates heavily (Fig. 13). The heavy accumulation of fuzzy stochastic damage stress causes the Domino effects in the neighboring areas. There is concentrative discreteness of fuzzy stochastic damage stress in the neighboring rock areas (Fig. 14), too. Therefore, these rock areas are of high danger of destabilization (Terzaghi 1962a).

The simulating results for the rock slope's working behaviors, including the fields of displacement, stress, damage and reliability, conform to each other based on fuzzy stochastic damage reliability approach. Hence, the fuzzy stochastic damage reliability approach can be applied in geo-engineering studies.

## 8. Discussions on fuzziness, stochastics, damage and reliability

With the fuzzification for  $\varpi$ , 'damage' has been gifted softer definition domain than

conventional way, such as modulus degradation. It means the engineers have more information to make rational policy for engineering application.  $\varpi$  has incorporated directly the development of mechanical fields of engineering cases. Thus, engineers can understand and apply it easily. After de-fuzzification, 'damage' becomes the distinct mechanical index that can express the damaged degree of structures or materials. It can be used for engineers to assess their safety state, too. The key models for this process are the fuzzy memberships functional.

After equivalent normalization, the damage variable will diminish evidently. Therefore, it can be deduced that  $\beta$  distribution definition on damage is conservative one. The corresponding numerical approach has somewhat confidence for geo-engineering application (Gao *et al.* 2016).

Reliability, based on the computation of fuzzy stochastic damage, expresses the safety state of engineering cases. Especially, the damage model here incorporates both the micro- and macro effects. This kind of assessment with uncertain definition permits engineers to make more comprehensive policy for engineering application. By the help of equivalent normalization, independence orthogonalization and standardization, many relevant factors are included in the simulation and analyses. These computation results offer for engineers more insights into the working behavior of engineering cases.

## 9. Conclusions

- With some primary concepts of fuzzy stochastic damage, two distributions of the fuzzy stochastic damage variable were developed based on fuzzy memberships functional. They, with linearity, have super fuzzy robustness. Their parameters have distinct mathematical definition and can be determined easily by micro- and macro-tests.
- The fuzzy stochastic damage numerical approach was developed and applied to Jianshan mine rock slope. The primary output fields, i.e., displacement, stress, damage variable characteristics, reliability and failure probability, were examined by their spatial distribution of and the results conformed to each other.
- Crucial characteristics of fuzzy stochastic damage such as statistical correlation, non-normal distribution, and fuzzy extensionality were assimilated into fuzzy stochastic damage numerical approach. The uncertainty of damage variable was improved. Two primary uncertain characteristics, namely fuzziness and stochastics of damage, were incorporated into the fuzzy stochastic damage model. Thus the model and the numerical approach established could be used with some confidence in the analyses of reliability and damage of geo-engineering.
- The theoretical model and the numerical algorithm developed in this paper are applicable ones for geo-engineering because the simulation results are the conservative ones that guarantee the high degree of security for the designed structures.
- Although the conventional mechanical fields could also indicate partly the performance statuses of the goal structures when compared with the results derived from the fuzzy stochastic damage numerical approach, the comprehensive fields of  $\beta^*$  and  $P_f^*$  are more helpful for engineers to assess efficiently the macro-safety state of the structures. Therefore, the comprehensive fields incorporating the stochastics and the fuzziness show super competitiveness for the engineers' design, assessment and decision-making.

## Acknowledgments

The research described in this paper was financially supported by the National Natural Science Foundation of China (Grant No: 51109118), Zhejiang Provincial Natural Science Foundation of China (Grant No: LY14E090001), United Development Project Foundation from Zhejiang Ocean University and Wenzhou University (Grant No: 21188004113), United Development Project Foundation from Zhejiang Ocean University and Hydrochina Huadong Engineering Corporation (Grant No: 21188004013) and Young Teachers Improvement Project Fund of Zhejiang Ocean University (Grant No: 11042101512).

## References

- ASTM E1570-11 (2011), Standard practice for computed tomographic (CT) examination, American Society for Testing and Materials (ASTM International); West Conshohocken, PA, USA.
- ASTM D7070-08 (2008), Standard test methods for creep of rock core under constant stress and temperature, American Society for Testing and Materials (ASTM International); West Conshohocken, PA, USA.
- ASTM D7012 (2014), Standard test methods for compressive strength and elastic moduli of intact rock core specimens under varying states of stress and temperatures, American Society for Testing and Materials (ASTM International); West Conshohocken, PA, USA.
- Bolton, M.D., Nakata, Y. and Cheng, Y.P. (2008), "Micro- and macro-mechanical behavior of DEM crushable materials", *Géotechnique*, **58**(6), 471-480.
- Bulleit, W.M. (2004), "Stochastic damage models for wood structural elements". Structures - A Structural Engineering Odyssey, *Structures 2001 - Proceedings of the 2001 Structures Congress and Exposition*, Washington, D.C., USA, June, pp. 1-9. [http://dx.doi.org/10.1061/40558\(2001\)183](http://dx.doi.org/10.1061/40558(2001)183) [On CD-ROM]
- Chowdhury, R.N., Tang, W.H. and Sidi, I. (1987), "Reliability model of progressive slope failure", *Géotechnique*, **37**(4), 467-481.
- Dzenis, Y.A. (1993), "Stochastic damage evolution in textile laminates", *Compos. Manuf.*, **4**(4), 187-193.
- Dzenis, Y.A. (1996), "Stochastic damage evolution modeling in laminates", *J. Thermoplastic Compos. Mater.*, **9**(1), 21-34.
- Farkas, L., Moens, D., Vandepitte, D. and Desmet, W. (2010), "Fuzzy finite element analysis based on reanalysis technique", *Struct. Safety*, **32**(6), 442-448.
- Gao, Y.F., Wu, D., Zhang, F., Lei, G.H. Qin, H.Y. and Qiu, Y. (2016), "Limit analysis of 3D Rock slope stability with non-linear failure criterion", *Geomech. Eng., Int. J.*, **10**(1), 59-76.
- Hearndon, J.L., Potirniche, G.P., Parker, D., Cuevas, P.M., Rinehart, H., Wang, P.T. and Horstemeyer, M.F. (2008), "Monitoring structural damage of components using an effective modulus approach", *Theor. Appl. Fract. Mech.*, **50**(1), 23-29.
- Ihara, C. and Tanaka, T. (2000), "Stochastic damage accumulation model for crack initiation in high-cycle fatigue", *Fatigue Fract. Eng. Mater. Struct.*, **23**(5), 375-380.
- Jaeger, J.C. (1971), "Friction of rocks and stability of rock slopes", *Géotechnique*, **21**(2), 97-134.
- Ju, J.W. and Tseng, K.H. (1995), "An improved two-dimensional micro-mechanical theory for brittle solids with randomly located interacting microcracks", *Int. J. Damage Mech.*, **4**(1), 23-57.
- Mahdaviifar, M.R. (2000), "Fuzzy information processing in landslide hazard zonation and preparing the computer system", *Landslides Res.*, **2**, 993-998.
- Pine, R.J., Owen, D.R.J., Coggan, J.S. and Rance, J.M. (2007), "A new discrete fracture modelling approach for rock masses", *Géotechnique*, **57**(9), 757-766.
- Rezaei, M., Monjezi, M. and Varjani, A.Y. (2011), "Development of a fuzzy model to predict flyrock in surface mining", *Safety Sci.*, **49**(2), 298-305.
- Rigatos, G. and Zhang, Q. (2009), "Fuzzy model validation using the local statistical approach", *Fuzzy Sets Syst.*, **160**(7), 882-904.

- Rinaldi, A., Kajcinovic, D. and Mastilovic, S. (2007), "Statistical damage mechanics and extreme value theory", *Int. J. Damage Mech.*, **16**(1), 57-76.
- Schuster, M.J., Juang, C.H., Roth, M.J.S. and Rosowsky, D.V. (2008), "Reliability analysis of building serviceability problems caused by excavation", *Géotechnique*, **58**(9), 743-749.
- Silberschmidt, V.V. (1998), "Dynamics of stochastic damage evolution", *Int. J. Damage Mech.*, **7**(1), 84-98.
- Silberschmidt, V.V. and Chabochej, L. (1994), "Effect of stochasticity on the damage accumulation in solids", *Int. J. Damage Mech.*, **3**(1), 57-70.
- Terzaghi, K. (1962a), "Measurement of stress in rock", *Géotechnique*, **12**(2), 105-124.
- Terzaghi, K. (1962b), "Stability of steep slopes on hard unweathered rock", *Géotechnique*, **12**(4), 251-270.
- Vili, P., Andrej, Ž., Jovan, T. and Ivan, P. (2014), "Comparison of three different methods for determination of damage in solid materials", *Mater. Des.*, **56**, 872-877.
- Wang, Y.J. (2012), "Super gravity dam generalized damage study", *Adv. Mater. Res.*, **479-481**, 421-425.
- Yang, X.L. and Pan, Q.J. (2015), "Three dimensional seismic and static stability of Rock slopes", *Geomech. Eng., Int. J.*, **8**(1), 97-111.
- Zeitoun, D.G. and Baker, R. (1992), "A stochastic approach for settlement predictions of shallow foundations", *Géotechnique*, **42**(4), 617-629.
- Zhang, W.H. and Valliappan, S. (1998a), "Continuum damage mechanics theory and application, part I, theory", *Int. J. Damage Mech.*, **7**(3), 250-273.
- Zhang, W.H. and Valliappan, S. (1998b), "Continuum damage mechanics theory and application, part II, application", *Int. J. Damage Mech.*, **7**(3), 274-297.
- Zhang, W.H. and Valliappan, S. (1990a), "Analysis of random anisotropic damage mechanics problems of rock mass, part I, probabilistic simulation", *Rock Mech. Rock Eng.*, **23**(2), 91-112.
- Zhang, W.H. and Valliappan, S. (1990b), "Analysis of random anisotropic damage mechanics problems of rock mass, part II, statistical estimation", *Rock Mech. Rock Eng.*, **23**(4), 241-259.
- Zhao, L.H., Cao, J.Y., Zhang, Y.B. and Luo, Q. (2015), "Effect of hydraulic distribution on the stability of a plane slide Rock slope under the nonlinear Barton-Bandis failure criterion", *Geomech. Eng., Int. J.*, **8**(3), 391-414.

**Appendix: Art of fuzzification on damage**

*DMI verification based on triaxial CT tests*

To verify the validation of DMI definition, the triaxial CT tests were implemented and the rock samples from stratum AQ of Jianshan mine was studied with the triaxial CT scanner system (Jaeger 1971). Fig. 15 shows the 7 tested rock samples. The tests standards meet ISRM suggested methods and ASTM requirements. ASTM standards are the main references in this paper for the rock samples’ drilling, laboratory treating, scanning and tri-axial loading (ASTM E1570-11 2011, ASTM D7070-08 2008, ASTM D7012 2014) because they can offer more specific indications for engineers and researchers.

The rock samples were drilled by XY-44B diamond cutter that was produced by China and Germany with the maximal drilled depth 2 200 mm and the maximal drilled diameter 1 000 mm. The coarse rock samples were treated in laboratory by hydraulic cutter BS355 that was produced by China and can produce normal samples with the accuracy  $\pm 1.5$  mm. The cylinder dimension of the 7 tested rock samples includes diameter 5 cm and height 10cm. During both CT scanning and triaxial loading processes, the temperature in the triaxial cabinet was kept at  $19 \pm 2^\circ\text{C}$  that was the measured temperature in situ got by XY-44B diamond cutter.

CT scanner system used here belongs to Key Laboratory of Geotechnical Mechanics and Engineering of the Ministry of Water in China (serial number: 2007S).

The strain-controlled triaxial system can offer the strain-stress curves during both CT scanning and triaxial loading processes. Table 4 shows the main parameters of triaxial CT scanner system.

Fig. 16 shows the typical strain-stress curves of these rock samples under different loading velocities.



Fig. 15 Rock samples of Jianshan mine

Table 4 Main parameters of SOMATOM Sensation 40 triaxial CT system

CT scanner		Triaxial system				
Minimal pixel size	Spatial resolution	Outline dimensions	Triaxial cabinet diameter	Extreme loading conditions		Vertical extension distance
				Vertical force	Confining pressure	
0.29 mm	$0.29 \times 0.29 \times 0.29 \text{ mm}^3$	Height: 62 cm Maximal diameter: 29.5 cm Minimal diameter: 21.5 cm	10cm	0-200 kN	0-60MPa	0-14 cm

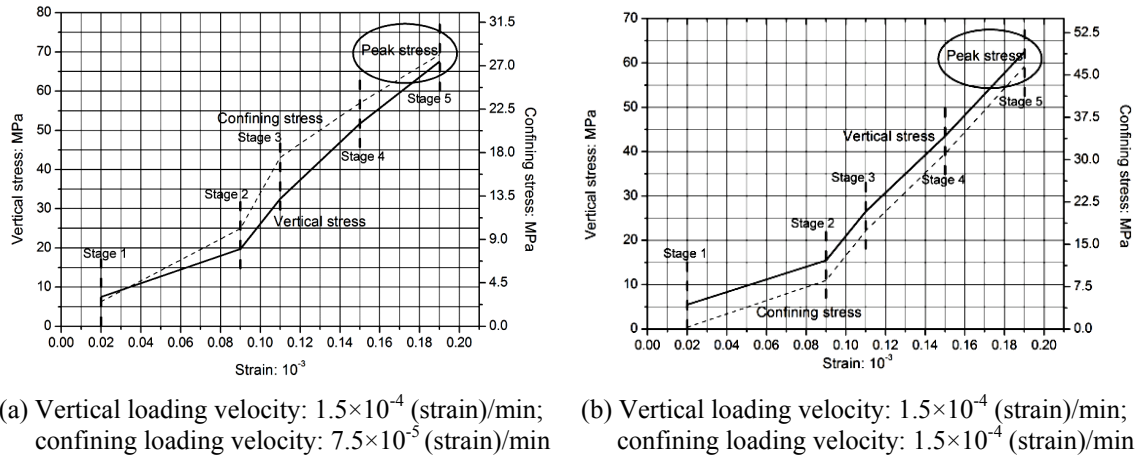


Fig. 16 Strain-stress curves of rock samples of Jianshan mine

Fig. 17 shows the typical CT slices of these rock samples. Their Hounsfield units (i.e.,  $H_u$ ), including the Hounsfield units of initial state (i.e.,  $H_{u0}$ ), were measured and computed. The representative micro-cracks of these rock samples were measured, too.

5 positions (from scanning stage 1 to stage 5) on the strain-stress curves were chosen to verify the relation between the rock samples' DMI and the corresponding  $H_u$ . Table 5 shows the comprehensive data on the triaxial CT tests.

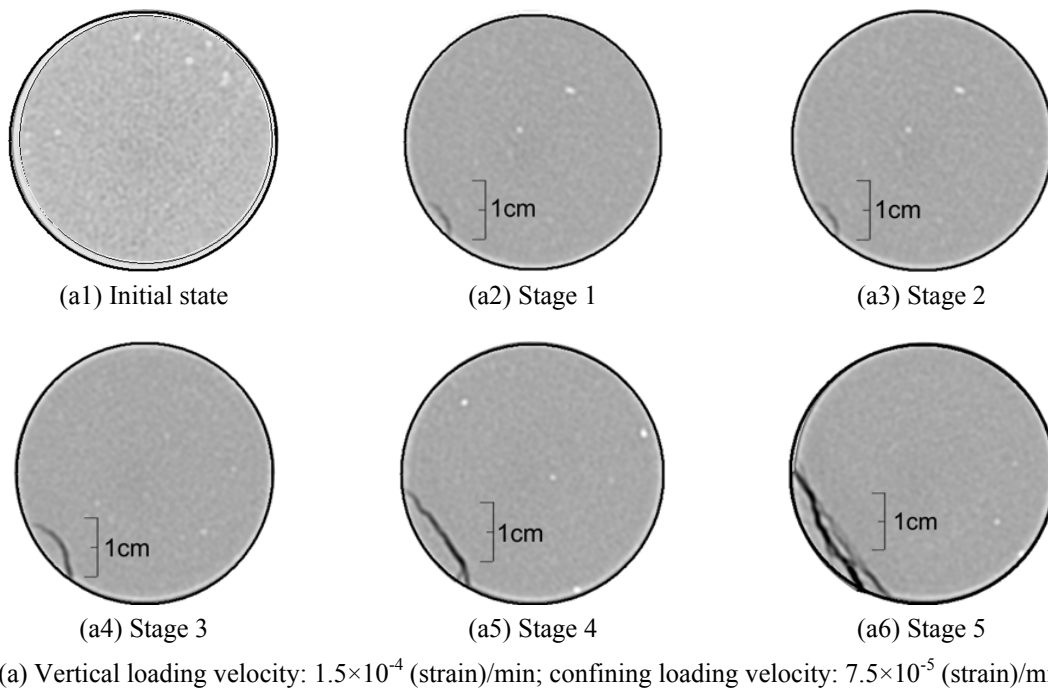
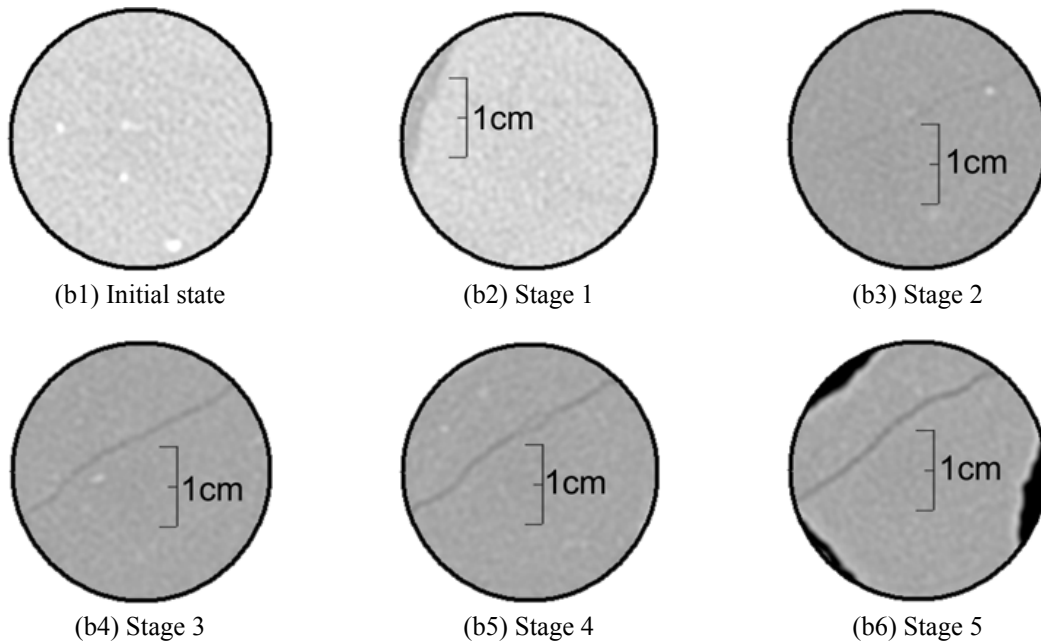


Fig. 17 CT slices of rock samples of Jianshan mine



(b) Vertical loading velocity:  $1.5 \times 10^{-4}$  (strain)/min; confining loading velocity:  $1.5 \times 10^{-4}$  (strain)/min

Fig. 17 Continued

Table 5 Triaxial CT tests data

Tests data												
Loading velocities : (strain)/min		Vertical: $1.5 \times 10^{-4}$ ; confining: $7.5 \times 10^{-5}$					Vertical: $1.5 \times 10^{-4}$ ; confining: $1.5 \times 10^{-4}$					
Scanning stage	Initial state	Stage1	Stage2	Stage3	Stage4	Stage5	Initial state	Stage1	Stage2	Stage3	Stage4	Stage5
Stress state: MPa; $\sigma_{11}$ , $\sigma_{22} = \sigma_{33}$	/	7.5, 2.55	19.7, 10.12	32.5, 17.52	51.7, 23.15	67.5, 27.16	/	5.5, 0.31	15.5, 8.61	26.5, 17.43	43.5, 31.06	62.5, 46.51
DMI values	/	1.61	1.36	1.21	0.83	0.7	/	1.31	1.69	1.87	2	2.15
Expectation values						Expectation values						
$H_u$	$H_{u0} = 1830.55$	1803.71	1780.42	1735.94	1699.31	1668.57	$H_{u0} = 1984.99$	1949.43	1916.79	1890.11	1836.79	1806.99
Mean square deviation values						Mean square deviation values						
	109.61	123.94	131.66	132.87	140.29	145.07	357.86	381.94	401.25	419.97	446.81	472.03
$\frac{H_{u0} - H_u}{H_{u0}}$	/	0.0147	0.0274	0.0517	0.0717	0.0885	/	0.0179	0.0344	0.0502	0.0747	0.0897
$\Omega$	/	0.05	0.25	0.45	0.65	0.85	/	0.05	0.25	0.45	0.65	0.85

The computation results of DMI, according to the triaxial CT tests, have close relation with the micro-defects' evolution that can be qualified by  $H_u$ . DMI defined here can reveal the geo-material's damage development characteristics (Terzaghi 1962). Especially, as macro-mechanical index that can be implanted easily into the numerical approaches, DMI  $\varpi$  can incorporate directly both the mechanical fields' development and the micro-defects' evolution. Thus, it is applicable for the reliability analyses of geo-engineering cases with uncertainty (including fuzziness and stochastics).

### *Fuzzy logical and topology*

The primary fuzzification criteria on  $\Omega$  include: the values of the fuzzy memberships functional (namely, the values of  $\Omega$ ) at the certain analytical domain keep the maximal ones or the minimal ones; input and output of fuzzy logics must be certain values; the fuzzy memberships functional should be simple ones for engineers.

According to the triaxial CT tests, 5-class development of material damage was established for the fuzzy membership. The linguistic variables for the corresponding fuzzy topology are (Table 5):

If  $0.08 \leq \frac{H_{u0} - H_u}{H_{u0}} \leq 0.1$ , then the fuzzy membership is 0.85 that means the material is damaged thoroughly;

If  $0.06 \leq \frac{H_{u0} - H_u}{H_{u0}} \leq 0.08$ , then the fuzzy membership is 0.65 that means the material is damaged seriously;

If  $0.04 \leq \frac{H_{u0} - H_u}{H_{u0}} \leq 0.06$ , then the fuzzy membership is 0.45 that means the material is damaged obviously;

If  $0.02 \leq \frac{H_{u0} - H_u}{H_{u0}} \leq 0.04$ , then the fuzzy membership is 0.25 that means the material is damaged moderately;

If  $\frac{H_{u0} - H_u}{H_{u0}} < 0.02$ , then the fuzzy membership is 0.05 that means the material is damaged slightly.

Especially, when  $\frac{H_{u0} - H_u}{H_{u0}} > 0.1$ , the fuzzy memberships keep the maximal one, namely, 1.

Here,  $\Omega$  is at the certain analytical domain.

According to the linguistic variables and triaxial CT tests data on  $\varpi$ , the tests' parameters  $a$ ,  $a'$ ,  $b$  and can be  $b'$  determined (Figs. 1 and 18). Especially,  $b$  and  $b'$  define the support of the fuzzy-set;  $a$  and  $a'$  describe not only the fuzzy-set core, but also the shape of the fuzzy membership functional. Thus, the whole fuzzy topology on damage variable has been established.

The robustness of fuzzy memberships functional can be computed as  $\frac{(2\zeta_{\varpi=1.495})(b-b')}{2(b-b')}$

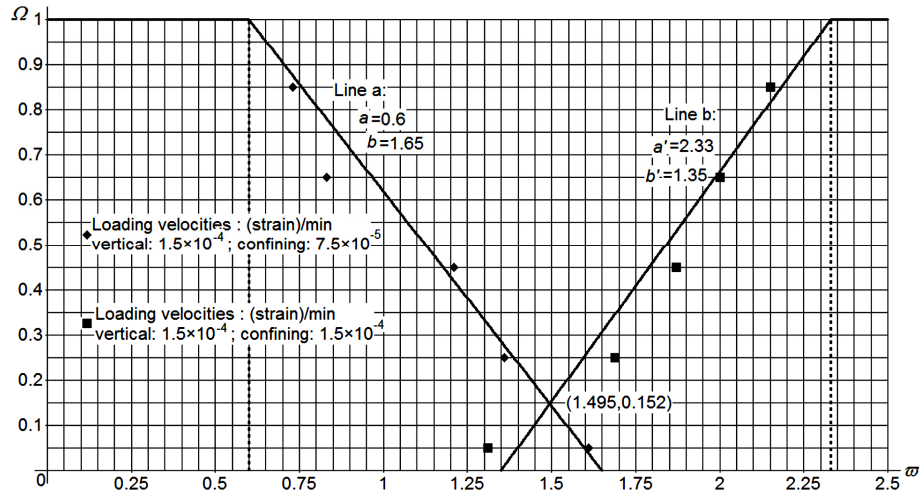


Fig. 18 Topological structure on fuzzy memberships functional

$\frac{2 \cdot 0.152 \cdot (1.65 - 1.35)}{2 \cdot (1.65 - 1.35)} = 0.152$  and the optimal values of robustness are 0.1–0.7 (MahdaviFar 2000).

As the input of fuzzy logics, DMI  $\sigma$  was determined according to the certain micro- and macro-mechanical tests. DMI has the certain mathematical expression and can be computed by the numerical approach developed in the work. The output of fuzzy logics was realized by defuzzification based on the gravity model approach. The outputted values of  $\Omega$  also have certain characteristics. Meanwhile, the fuzzy memberships functional established here are the simple and applicable ones for engineers' implementation.

**Notation**

$\tilde{A}$	fuzzy subset
$a, a'$	test parameters
$\mathbf{B}$	transformation vector
$b, b'$	test parameters
$\mathbf{C}$	covariance matrix
$\tilde{C}$	fuzzy set of physical parameters
$c$	cohesive strength
$\mathbf{D}$	stochastic characteristics matrix
$d$	iterative step size
$\mathbf{E}$	stochastic characteristics matrix
$E$	Young's modulus
$e_{s,f}$	fuzzy stochastic strain tensor
$e_{a'}$	stochastic strain tensor
$F_{\Omega}^f$	generalized cumulative distribution function (GCDF)
$f$	fuzzy coverage
$\mathbf{f}_{s,f}$	fuzzy stochastic body force vector
$\mathbf{f}_{a'}$	probabilistic body force vector
$f_{\Omega}^f$	generalized probabilistic density function (GPDF)
$g_{a^*}$	ultimate status function
$\mathbf{H}$	transformation matrix
$H_u$	Hounsfield unit
$H_{i0}$	initial Hounsfield unit
$\mathbf{h}$	orthogonal vector
$J_2$	second invariable of deviatoric stress tensor
$\tilde{L}$	fuzzy set of loading conditions
$N$	size of fuzzy memberships functional
$n$	size of stochastic parameters
$\tilde{P}$	fuzzy set of boundary conditions

$P_f^*$	failure probability
$p, q$	parameters for $\beta$ function
$s$	stochastic coverage
$\mathbf{T}$	transformation matrix
$\mathbf{U}_{s,f}$	fuzzy stochastic nodal displacement vector
$\mathbf{U}_{\alpha'}$	probabilistic nodal displacement vector
$\nu$	Poisson ratio
$\mathbf{x}, X, X', Y^*, Z$	stochastic vector
$x_i, x'_i, y_i, z_i$	stochastic parameters
$y_1, y_2$	probabilistic cumulative distribution function vector
$\boldsymbol{\alpha}$	negative gradient direction vector
$\alpha'$	stochastic subset
$\alpha_i$	direction cosine component
$\beta^*$	fuzzy stochastic damage reliability index
$\beta(p, q)$	$\beta$ distribution function
$\Gamma$	fuzzy analytical domain
$\gamma$	unit weight
$\delta_{x'_i}, \delta_{z_i}$	mean square deviation
$\varepsilon$	accuracy
$\mu_{x'_i}, \mu_{z_i}$	expectation
$\Xi$	single fuzzy space
$\xi(s, f)$	generalized uncertain subset
$\mathcal{O}$	generalized uncertain space
$\rho_{x_i, x_j}$	correlation coefficient
$\boldsymbol{\sigma}_{s,f}$	fuzzy stochastic stress tensor
$\boldsymbol{\sigma}_{\alpha'}$	stochastic stress tensor
$\sigma_m$	hydrostatic pressure
$\sigma_{xx}$	normal stress components
$\Phi$	standard normal cumulative distribution function (CDF)

$\varphi$	internal friction angle
$\phi$	standard normal probabilistic density function (PDF)
$\Psi$	single random space
$\Psi_1, \Psi_2$	probabilistic space of independent $\beta$ distribution
$\Omega$	damage variable
$\omega$	generalized probabilistic integral variable
$\omega_\Gamma$	generalized probabilistic integral function
$\Lambda_{\alpha'}$	probabilistic set
$\nabla$	gradient operator
$\nabla g_{\alpha^*}$	ultimate status function gradient
$\varpi$	damage measuring index (DMI)
$\zeta_{\varpi \in \Gamma}$	fuzzy membership functional